JOURNAL OF COLLOID SCIENCE 20, 353–375 (1965)

THE PERMEABILITY OF SOAP FILMS TO GASES[1]

H. M. Princen and S. G. Mason

Pulp and Paper Research Institute of Canada and Department of Chemistry, McGill University, Montreal 2, Canada

Received August 13, 1964; revised January 2, 1965

Abstract

A stabilized gas bubble resting at a gas/liquid interface decreases in size owing to outward diffusion of gas across the liquid film at the top of the bubble. Brown, Thuman, and McBain used the rate of shrinkage to calculate the permeability of the film to air but the theory employed is inexact.

An improved theory is presented here which takes into account the exact shape of the bubble and, in the case of multicomponent gases such as air, the changing composition. It is shown that after a short period the composition of the gas in the bubble adjusts itself so that the observed permeability becomes constant.

If the equilibrium thickness of the film is known, the method can be used to measure the permeability of the monolayers on both sides of the film.

The experimental results support the modified theory. The method appears to produce accurate and reproducible values of the film permeability, and values for a number of gases at various concentrations of surfactant, at various temperatures, and with added electrolytes are presented.

Introduction

Mass transport across thin liquid films is of interest in a number of problems in colloid science, such as retardation of evaporation (1) and foam stability (2, 3). In this paper we describe an extension of the method of Brown *et al.* (4) of measuring the permeability of soap films to gases from the deflation of a gas bubble floating at the free surface of a soap solution. The shrinkage is caused by diffusion of the gas from the region of excess pressure inside the bubble across the exposed film. On the assumption that the bubble is spherical and exactly half immersed in the liquid, the following relation between the bubble radius r and time t was derived (4).

$$-\frac{dr^2}{dt} = \frac{4\gamma}{\bar{p}}\,k, \qquad [1]$$

where γ is the surface tension and $\bar{p}$ the atmospheric pressure; k is the film permeability defined by

$$-\frac{dN}{dt} = kA\Delta C, \qquad [2]$$

[1] This work was supported by the Petroleum Research Fund (PRF Grant 1214-A4).

where N is the moles of gas diffusing through the film at the top of the bubble of area A, and ΔC is the difference in concentration of gas across the bubble film in moles per cubic centimeter.

With air bubbles it was found that values of k calculated from [1] decreased with time. Brown *et al.* (4) suggested that this behavior could result from a nonspherical bubble shape, from changing composition of the air inside the bubble as a result of selective diffusion of oxygen, or from a slow change in film structure. In the following part a corrected version of [1] is developed based on the exact shape of the bubble and the use of equilibrium films. It is also demonstrated that the explanation based on selective diffusion is implausible. Further improvements in the theory and methods presented below allow for the volatility of the liquid and permit the use of bubble dimensions which can be accurately measured.

Theoretical Part

1. Film Permeability

A liquid film, stabilized by the addition of an appropriate surfactant, can be schematically represented as in Fig. 1*a*. A central, liquid layer of thickness h is bounded by two monolayers of thickness δ, consisting of adsorbed surfactant molecules and possibly a few hydration layers of solvent molecules. Driven by a positive pressure difference $\Delta p = p_1 - p_2$ or a concentration difference $\Delta C = C_1 - C_2$, a gas will diffuse across the film from left to right. In the steady state the gas concentration in the central liquid layer drops linearly from C_1' to C_2', so that the flux across any plane in this layer is

$$\frac{dN}{dt} = DA\,\frac{C_1' - C_2'}{h}, \qquad [3]$$

where D is the diffusion coefficient of the gas in the liquid phase.

If the equilibrium concentrations in the liquid corresponding to C_1 and C_2 in the gas phase are denoted by $\bar{C}_1$ and $\bar{C}_2$, Henry's law may be written

$$\bar{C}_1 = HC_1\,;\ \bar{C}_2 = HC_2\,, \qquad [4]$$

where H is the Ostwald coefficient of gas solubility.

In general $C_1' < \bar{C}_1$ and $C_2' > \bar{C}_2$ because of the finite rate of permeation of the gas through each monolayer, given by

$$\frac{dN}{dt} = k_{ML}A(\bar{C}_1 - C_1') \qquad [5]$$

and

$$\frac{dN}{dt} = k_{ML}A(C_2' - \bar{C}_2), \qquad [6]$$

where k_{ML} is the monolayer permeability. In [5] the driving force ($\bar{C}_1 -$

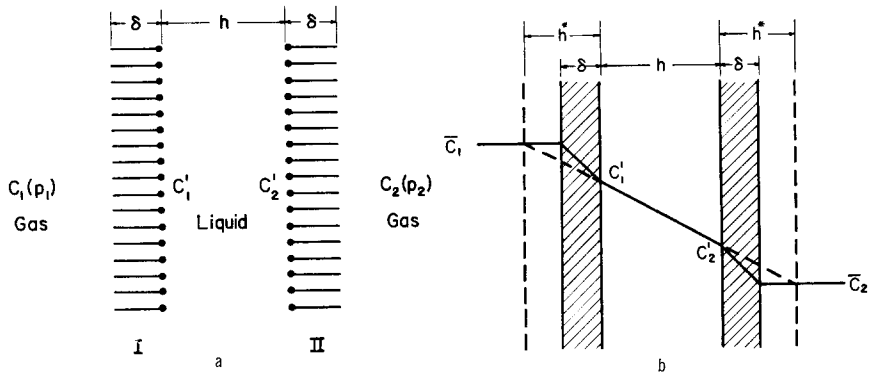

FIG. 1. (*a*) Thin liquid film bounded by two monolayers of surfactant molecules (schematic). (*b*) Variation of the gas concentration across a thin liquid film and across the equivalent film consisting of bulk liquid only with zero resistance to permeation at the surfaces.

C_1') is the difference in the effective gas concentrations in the phases *outside* the monolayer. Thus the definition of k_{ML} does not involve any assumption concerning the inaccessible gas concentration in the monolayer itself.

Although one might introduce a diffusion coefficient $D_{ML} = k_{ML}\delta$, it has been pointed out by Blank (5, 6) that this quantity is not a diffusion coefficient in the true sense since it depends on the monolayer thickness.

In the steady state the three fluxes given by [3], [5], and [6] are equal, from which one obtains

$$C_1' - C_2' = \frac{hH}{h + 2D/k_{ML}}(C_1 - C_2). \qquad [7]$$

Finally, by combining [2], [3], and [7] one finds

$$k = \frac{DH}{h + 2D/k_{ML}}. \qquad [8]$$

Two limiting cases of [8] are of interest:

1. $2D/k_{ML} \ll h$, yielding

$$k = \frac{DH}{h}. \qquad [9]$$

In this situation, approached in thick films, the rate of permeation is controlled by the liquid layer.

2. $2D/k_{ML} \gg h$, which leads to

$$k = \frac{Hk_{ML}}{2}. \qquad [10]$$

Here the permeation is controlled by the monolayers. This will presumably occur in very thin films like the Perrin first-order black films.[2]

Equations similar to [8] have been derived by van Amerongen (9), and Korvezee and Mol (10) for the permeation of rubber membranes by gases and of polymer membranes by water vapor. Although de Vries (2) suggested its application to the diffusion of gases through soap films, he actually used [9] because k_{ML} was not known.

It is useful to write [8] in the form

$$k = \frac{DH}{h + 2h^*}, \qquad [11]$$

where

$$h^* = \frac{D}{k_{ML}}. \qquad [12]$$

It is readily shown that h^* equals the thickness of a water layer with the same permeability as the monolayer of thickness δ, as shown in Fig. 1*b*, where the real film and the corresponding concentration drop are drawn as solid lines. For simplicity it is assumed that the gas concentration in the monolayer varies linearly. The dashed lines indicate the surfaces of a film of equal permeability, but consisting of bulk liquid only. The latter imaginary film has a total thickness $h + 2h^*$, and the concentration of the gas in this film drops linearly from $\bar{C}_1$ at the left to $\bar{C}_2$ at the right. To avoid discontinuities in gas concentration, the effective concentrations $\bar{C}_1$ and $\bar{C}_2$ have been used outside the film in Fig. 1*b*, instead of the actual concentrations C_1 and C_2. For the same reason the concentration in the monolayer is shown to vary between $\bar{C}_1$ and C_1'.

2. Diffusion from Bubble

In this section the exact shape of the bubble (11), illustrated in Fig. 2, is taken into account in applying [2]. The bubble top is spherical and of radius R and height h_{cap}. The circle of contact where the free bubble and bulk interfaces meet with a common slope is of radius x_c. The free bubble interface has the shape of a sessile drop and is characterized by the dimensionless

[2] In the absence of a universal agreement on equilibrium films, we follow the nomenclature of Duyvis (7), which is based on the modern view that there may be two minima in the potential energy versus thickness curve. A Perrin first-order black film corresponds to the primary minimum, and consists of two layers of surfactant molecules and possibly a few layers of water molecules. The thicker second-order equilibrium film corresponds to the secondary minimum; its thickness is determined by the equilibrium between the electrostatic repulsion of the electrical double layers, the van der Waals attraction, and the hydrostatic suction in the film. These films have previously been termed the second and first black film, respectively, based on the chronological order in which they appear in a draining film. Sheludko (8) refers to the thinner film as "Perrin film."

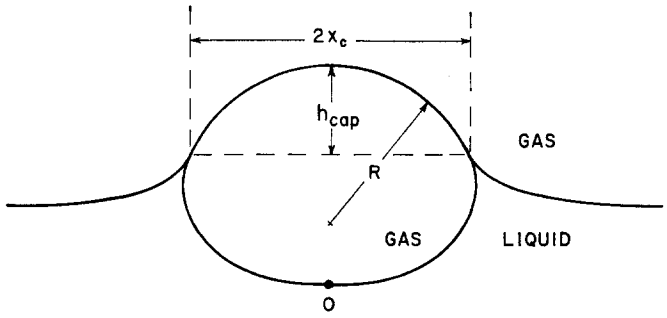

FIG. 2. Parameters for describing exact shape of a gas bubble at a horizontal gas-liquid interface. The radius of curvature of the interface at point O is b.

parameter (11) $\beta = cb^2$, where b is the radius of curvature at the bottom of the bubble, $c = (dg/\gamma)$, d and γ are the density and surface tension of the liquid, and g is gravity.

If the gas is assumed to be ideal and the liquid phase to have a vapor pressure p_L, the rate of deflation of the bubble may be written

$$-\frac{dN}{dt} = -\frac{\bar{p} - p_L}{\mathbf{R}T}\frac{dV}{dt} = -\frac{4\pi r^2}{\mathbf{R}T}(\bar{p} - p_L)\frac{dr}{dt}. \qquad [13]$$

Here V is the volume of the bubble, r the radius of a sphere of the same volume as the deformed bubble, $\mathbf{R}$ the gas constant, and T the absolute temperature.

Beyond the circle of contact the distance between the free bubble and bulk interfaces increases so rapidly that all the gas diffusion may be assumed to occur through the film. Its surface area is

$$A = 2\pi R h_{cap}, \qquad [14]$$

while the excess concentration of gas in the bubble is

$$\Delta C = \frac{\Delta p}{\mathbf{R}T} = \frac{4\gamma}{R\mathbf{R}T}. \qquad [15]$$

Substituting for dN/dt, A, and ΔC in [2] yields

$$-\frac{dr^2}{dt} = \frac{4\gamma k\alpha}{\bar{p} - p_L}. \qquad [16]$$

Except for p_L and $\alpha = h_{cap}/r$ this is equivalent to [1]. The dimensionless factor α, however, is important since it can vary from 0 for very small bubbles to 1.260. It should also be noted that r is not directly measurable.

Multiplying [16] by c gives

$$-\frac{d\beta_0}{dt} = \frac{4\ dgk\alpha}{\bar{p} - p_L}, \qquad [17]$$

where $\beta_0 = cr^2$. Equation [17] is convenient since the bubble parameters α and β_0 are dimensionless and can be computed from measurable quantities; $x_c\sqrt{c}$ is particularly useful for this purpose.

Although the essential bubble shape data have been given before (11), their form is inconvenient for the present purpose. From a revised table we have selected the necessary data in Table I; their use is explained later. To facilitate linear interpolation $\beta_0^{1/2}$, instead of β_0, is recorded. From [16] and Table I it is immediately clear that $-dr^2/dt$ decreases as the bubble shrinks since α decreases with r; this is the reason for the apparent decrease in k if [1] is employed.

For very large bubbles the shape approaches that of a hemisphere (11) with radius $R = h_{cap} = 1.260\, r$, and [16] reduces to

$$-\frac{dR^2}{dt} = \frac{8\gamma k}{\bar{p} - p_L}. \qquad [18]$$

Very small bubbles, on the other hand, remain nearly spherical (11) of radius r and having a small contact area at the top with $R = 2r$. It can be shown that here $\alpha = cr^2/3$, which yields from [16]

$$-\frac{d \ln r}{dt} = \frac{2\, dgk}{3(\bar{p} - p_L)}. \qquad [19]$$

Because in most experiments of Brown *et al* (4) α was about 0.15, the values of k they obtained from [1] are too small by a factor of five to ten, whereas application of [19] to their systems would have yielded values less than 20% in error.

3. *Diffusion of Binary Gases*

In this section we consider the behavior of a two-component gas in which each of the two components A and B has a different k. For simplicity we consider a spherical bubble in an infinite atmosphere and an equilibrium film of nonvolatile liquid.

For a one-component gas diffusing from a spherical bubble Eq. [2] leads to

$$-\frac{dr^2}{dt} = \frac{8\gamma}{\bar{p}} k. \qquad [20]$$

For a binary gas the total pressure in the bubble is p, and the partial pressures and mole fractions are p_A, p_B, x_A, and x_B; in the atmosphere the same quantities are $\bar{p}$, $\bar{p}_A$, $\bar{p}_B$, $\bar{x}_A$, and $\bar{x}_B$, which are all constant. If the total number of moles in the bubble is $N = N_A + N_B$, then $x_A = N_A/N$ and $x_B = N_B/N$.

The excess pressure in the bubble

$$\Delta p = p - \bar{p} = 4\gamma/r$$

TABLE I

Parameters for Calculating the Film Permeability

β	0.125	0.25	0.5	0.75	1	1.5	2
$x_c\sqrt{c}$	0.1287	0.2336	0.3991	0.5274	0.6324	0.7985	0.9277
$\beta_0^{1/2}$	0.3405	0.4665	0.6264	0.7356	0.8196	0.9465	1.0419
α	0.0383	0.0702	0.1205	0.1589	0.1897	0.2368	0.2721
β	2.5	3	3.5	4	5	6	7
$x_c\sqrt{c}$	1.0335	1.1231	1.2008	1.2695	1.3866	1.4841	1.5678
$\beta_0^{1/2}$	1.1187	1.1830	1.2384	1.2872	1.3700	1.4387	1.4976
α	0.3000	0.3230	0.3424	0.3592	0.3869	0.4092	0.4277
β	8	9	10	12	14	16	18
$x_c\sqrt{c}$	1.6410	1.7060	1.7645	1.8665	1.9533	2.0288	2.0956
$\beta_0^{1/2}$	1.5491	1.5949	1.6361	1.7079	1.7691	1.8224	1.8697
α	0.4435	0.4572	0.4693	0.4897	0.5065	0.5207	0.5330
β	20	24	28	32	36	40	45
$x_c\sqrt{c}$	2.1555	2.2595	2.3476	2.4240	2.4914	2.5518	2.6194
$\beta_0^{1/2}$	1.9121	1.9859	2.0486	2.1029	2.1511	2.1943	2.2428
α	0.5437	0.5618	0.5766	0.5891	0.5998	0.6092	0.6194
β	50	56	64	70	80	90	100
$x_c\sqrt{c}$	2.6797	2.7447	2.8212	2.8726	2.9490	3.0164	3.0766
$\beta_0^{1/2}$	2.2860	2.3328	2.3879	2.4250	2.4802	2.5291	2.5728
α	0.6284	0.6378	0.6486	0.6557	0.6661	0.6749	0.6826

is the sum of the excess partial pressures

$$\Delta p = \Delta p_A + \Delta p_B = (p_A - \bar{p}_A) + (p_B - \bar{p}_B).$$

It is assumed that r is large enough to make $\Delta p \ll \bar{p}$. Initially $x_A = \bar{x}_A$, $x_B = \bar{x}_B$, and $r = r_0$. Assuming further that the diffusions of A and B are independent one may then write

$$-\frac{dN_Z}{dt} = k_Z A \Delta C_Z = \frac{4\pi r^2}{\mathbf{R}T} k_Z \Delta p_Z, \qquad Z \equiv A, B. \qquad [21, 22]$$

Adding [21] and [22] yields

$$-\frac{dN}{dt} = \frac{4\pi r^2}{\mathbf{R}T} (k_A \Delta p_A + k_B \Delta p_B). \qquad [23]$$

Because of [13] this is equivalent to

$$-\frac{dr}{dt} = \frac{1}{\bar{p}}\,(k_A\,\Delta p_A + k_B\,\Delta p_B), \qquad [24]$$

or

$$-\frac{dr^2}{dt} = \frac{8\gamma}{\bar{p}}\left(k_A\,\frac{\Delta p_A}{\Delta p} + k_B\,\frac{\Delta p_B}{\Delta p}\right) = \frac{8\gamma}{\bar{p}}\,k_{AB}. \qquad [25]$$

Equations [25] and [20] are identical, except that k_{AB} may be time dependent as suggested by Brown *et al.* (4).

The composition of the gas in the bubble is, in general, a function of time given by

$$\frac{dx_A}{dt} = \frac{1}{N}\left(\frac{dN_A}{dt} - x_A\,\frac{dN}{dt}\right) = \frac{4\pi r^2}{NRT}\,[-k_A\,\Delta p_A + x_A(k_A\,\Delta p_A + k_B\,\Delta p_B]. \qquad [26]$$

Since $NRT = \bar{p}V = 4\pi r^3\bar{p}/3$, [26] reduces to

$$\frac{dx_A}{dt} = \frac{d(\Delta x_A)}{dt} = \frac{3}{r\bar{p}}\,[-k_A\,\Delta p_A + x_A(k_A\,\Delta p_A + k_B\,\Delta p_B)], \qquad [27]$$

where $\Delta x_A = x_A - \bar{x}_A$.

The excess partial pressures are given by

$$\Delta p_Z = x_Z p - \bar{x}_Z\bar{p}\,, \qquad Z \equiv A, B. \qquad [28, 29]$$

Equations [25] and [27], in combination with [28] and [29], describe the time dependence of the system completely.

As long as $|\,\Delta x_A| \ll \bar{x}_A$, one may write

$$\Delta p_A = \bar{x}_A\Delta p + \Delta x_A\bar{p}, \qquad [30]$$

and

$$\Delta p_B = \bar{x}_B\Delta p - \Delta x_A\bar{p}. \qquad [31]$$

If, in addition, $r \approx r_0$ [27] becomes

$$\frac{d(\Delta x_A)}{dt} = -\frac{3}{r_0}\left[\frac{\Delta p}{\bar{p}}\,\bar{x}_A\,\bar{x}_B(k_A - k_B) + (\bar{x}_A k_B + \bar{x}_B k_A)\Delta x_A\right]. \qquad [32]$$

Equation [32] integrates to

$$\ln\left(1 + \frac{u}{v}\,\Delta x_A\right) = -\frac{3ut}{r_0}\,, \qquad [33]$$

where $u = \bar{x}_A k_B + \bar{x}_B k_A$, and $v = \dfrac{\Delta p}{\bar{p}}\,\bar{x}_A\bar{x}_B(k_A - k_B)$; or alternatively

$$\Delta x_A = \frac{v}{u}\,[\exp\,(-3ut/r_0) - 1]. \qquad [34]$$

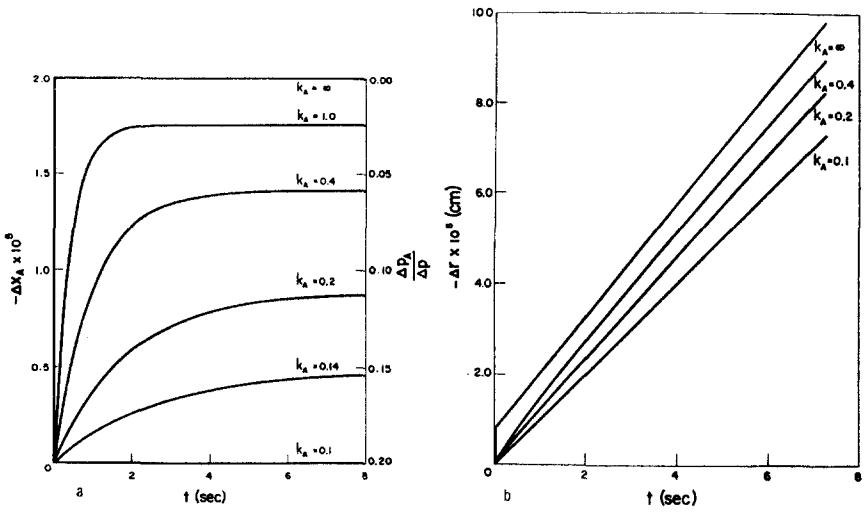

FIG. 3. Time dependence of Δx_A , $\Delta p_A/\Delta p$, and Δr for a spherical bubble in a binary gas immediately after formation, ($r_0 = 1$ cm.; $k_B = 0.1$ cm./sec.; $\gamma = 25$ dynes/cm.; $\bar{x}_A = 0.2$; $\bar{x}_B = 0.8$). Note that when $k_A = k_B = 0.1$ cm./sec., no change in Δx_A and $\Delta p_A/\Delta p$ takes place, whereas these changes are instantaneous when $k_A = \infty$.

Substituting for Δx_A , Δp_A , and Δp_B in [24] renders it soluble, with the result

$$\Delta r = r - r_0 = \left[(k_A - k_B) \frac{v}{u} - \frac{\Delta p}{\bar{p}} (\bar{x}_A k_A + \bar{x}_B k_B) \right] t + (k_A - k_B) \frac{v r_0}{3u^2} [\exp(-3ut/r_0) - 1]. \quad [35]$$

As an example the variations with time of Δx_A , $\Delta p_A/\Delta p$, and Δr calculated from [34], [30], and [35] are shown in Fig. 3 for $r_0 = 1$ cm., $\gamma = 25$ dynes/cm., $\bar{p} = 10^6$ dynes/cm.^{2}, $k_B = 0.1$ cm./sec., and different values of k_A . Air is considered to be the diffusing gas by choosing $\bar{x}_A = 0.2$ and $\bar{x}_B = 0.8$.

It is clear that there is a rapid change in composition which is small but important in its effect on the driving forces for diffusion Δp_A and Δp_B . It is also evident that for the times considered in Fig. 3, [34] and [35] are nearly exact because of the small changes in r and x_A . The excess mole fraction will rapidly reach the value as given by [34] for large t:

$$\Delta x_A = -v/u. \quad [36]$$

If this value is inserted in [30] and [31], one finds

$$\frac{\Delta p_A}{\Delta p} = \frac{\bar{x}_A k_B}{\bar{x}_A k_B + \bar{x}_B k_A}, \quad [37]$$

$$\frac{\Delta p_B}{\Delta p} = \frac{\bar{x}_B k_A}{\bar{x}_A k_B + \bar{x}_B k_A} . \qquad [38]$$

The significance of this becomes clear upon substituting for these excess partial pressures in [21] and [22], from which it is seen that

$$\frac{-dN_A/dt}{-dN_B/dt} = \bar{x}_A/\bar{x}_B , \qquad [39]$$

which is approximately equal to x_A/x_B .

Thus at this stage the molecules of A and B diffuse out from the bubble in numbers nearly in the same ratio as their respective mole fractions in the bubble, so that the mole fractions subsequently change very slowly. It can also be shown that [36], [37], and [38] remain valid as the bubble shrinks further, so that Δx_A , Δp_A , and Δp_B vary linearly with Δp, which, in turn, varies as r^{-1}.

Substituting [37] and [38] into [25] leads to the conclusion that after a negligibly short time k_{AB} reaches a constant value given by

$$k_{AB} = \frac{1}{\bar{x}_A/k_A + \bar{x}_B/k_B} . \qquad [40]$$

Then the diffusion process is indistinguishable from that of a pure gas. It can be shown that for a multicomponent gas the equivalent of [40] is

$$k_{gas} = \frac{1}{\sum_i \bar{x}_i/k_i} . \qquad [41]$$

If the liquid has an appreciable vapor pressure p_L , the pressure $\bar{p}$ in [24] is replaced by $\bar{p} - p_L$, while the mole fractions in [40] and [41] are those in the dry gas.

Although the complicated geometry of a gas bubble at a gas-liquid interface does not allow an exact treatment of the diffusion process, the essential results will be the same as above.

Experimental Part

The experiments are conducted in a hermetically sealed thermostatted cell using techniques of forming and observing single gas bubbles described in greater detail elsewhere (12). Before an experiment is started, the solution is saturated by flushing the cell for at least 40 hours with the gas, which, in turn, is presaturated with water vapor by passing it through a bubbler. The cell is closed, a gas bubble is formed at the interface, and the bubble film is allowed to drain to the equilibrium thickness.

The bubble, illuminated by a horizontal parallel transmitted light beam, is photographed at convenient intervals by means of a 35 mm. Praktica single-lens reflex camera equipped with an extension tube and a 75 mm.

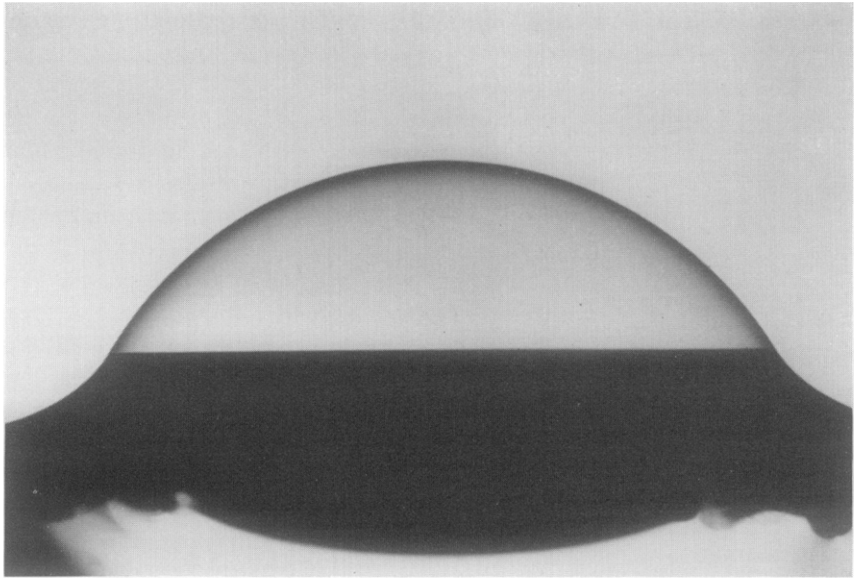

FIG. 4. Typical photograph of a gas bubble at a gas-liquid interface in horizontally transmitted light.

Berthiot Cinor lens. As shown in Fig. 4 the sharp boundary between the transparent film and the lower part of the bubble is the circle of contact. This length ($2x_c$) is measured directly on the negative by means of a traveling microscope.

From photographs of pendent drops in the same cell $\sqrt{c}$ is obtained using Fordham's tables (13), thus yielding the dimensionless parameter $x_c\sqrt{c}$ for each photograph. Subsequently, Table I is employed to find the corresponding values of $\beta_0^{1/2}$ and α by linear interpolation.

Two methods of calculating k from the time dependence of β_0 and α are used:

Method I. This makes use of the integrated form of [17]

$$\beta_0(0) - \beta_0(t) = K \int_0^t \alpha \, dt, \qquad [42]$$

where

$$K = \frac{4dgk}{\bar{p} - p_L}. \qquad [43]$$

The time limits are the first and last photographs in a run, and the integral is evaluated graphically.

Method II. Equation [17] is used directly with values of $-d\beta_0/dt$ calculated

by finite differences for each pair of consecutive observations in a run, and employing the mean value of α. A number of values of K are thus obtained, and the average $\bar{K}$ is substituted in [43] to yield k.

Method I yields an average value of k, and possible changes in the permeability are not detected. If such changes do occur, e.g., in draining films, Method II reveals them by a trend in the individual values of K.

The experimental system also allows the drainage process in the film prior to equilibrium to be observed. After the bubble is formed, white light *transmitted* by the film exhibits brilliant interference colors. With monochromatic light a succession of maxima and minima in the transmitted intensity occurs. These variations can be observed conveniently on the ground-glass viewer of the camera and are especially striking for light having an angle of incidence close to 90°, i.e., along the outer edge of the film (the dark arc in Fig. 4). For transmitted white light we have developed a theory which correlates the observed colors and the film thickness (14). Roughly speaking, these colors are complementary to the familiar interference colors in light *reflected* by a liquid film. The theory is useful only for relatively thick films (>1000 A.), whereas the equilibrium films are much thinner.

Results

1. Preliminary Experiments

In the early experiments with air a solution forming extremely stable bubbles was used (15), consisting of 80 g. of sucrose and 52 ml. of glycerine added to 100 ml. of a 2% aqueous Aerosol OT solution. The interference colors in the film after formation of a bubble indicated that the film drained very uniformly. After about an hour the film was grey, corresponding to a thickness of about 1400 A. Further drainage finally resulted in a black spot[3] at the top which increased in size until it covered the whole film. Then the film was probably a second-order equilibrium film.

Photographing of the bubble was started at least 20 hours after forming it to be reasonably certain of an equilibrium film, by which time the bubble had already shrunk appreciably. Photographs were then taken during the day at intervals varying between 1 and 2 hours; observations were resumed the following day and the bubble was finally destroyed. In this way two runs were obtained from a single bubble, each consisting of between six and ten photographs. This procedure was followed with four bubbles of different initial sizes; from the fifth bubble only one run was obtained.

[3] The term "black spot" is commonly used to describe a patch of film much thinner than the surrounding film. In reflected light this patch shows up as a hole because of its small reflection coefficient. Since observations being described here were made in transmitted light, the black spot showed up as a light area because of its higher transmission coefficient.

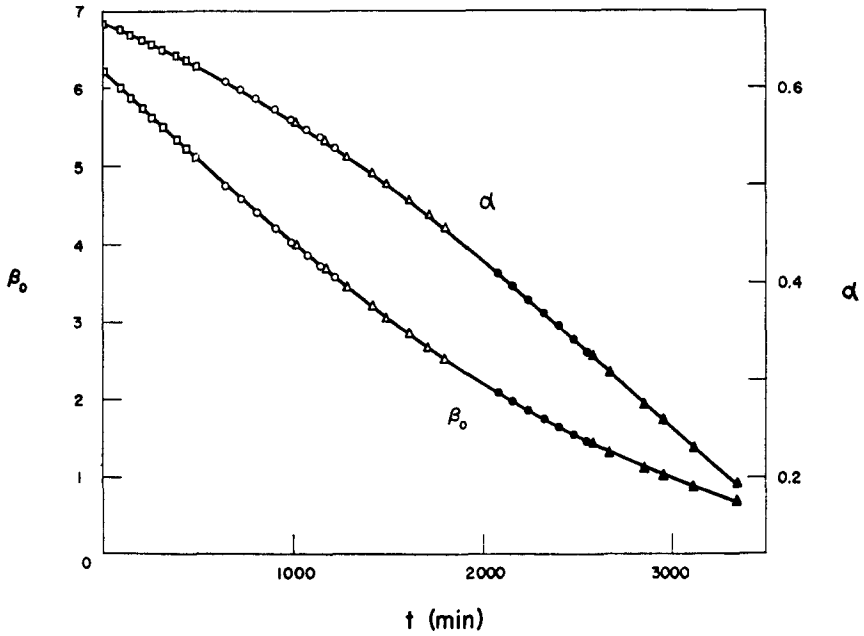

FIG. 5. Time dependence of β_0 and α for an air bubble at the surface of Kuehner's solution (see text). *Open squares:* run 4; *open circles:* run 3a; *open triangles:* run 1a; *solid circles:* run 3b; *solid triangles:* run 1b.

TABLE II

Permeability of an Equilibrium Film to Air

Liquid Phase: Kuehner's Solution

$T = 23.0 \pm 0.05°C.$; $\sqrt{c} = 6.77$ cm.$^{-1}$; $d = 1.202$ g./cm.^{3}, $p_L = 2.0 \times 10^4$ dynes/cm.^{2}.

Bubble	Run	$\frac{\bar{p} - p_L}{4\,dg}$ (cm.)	METHOD I $\beta_0(0)$	METHOD I $\beta_0(t)$	METHOD I $\int_0^t \alpha\,dt \times 10^{-3}$ sec.	METHOD I $K \times 10^4$ (sec.$^{-1}$)	METHOD I $k \times 10^2$ (cm./sec.)	METHOD II $\bar{K} \times 10^4$ (sec.$^{-1}$)	METHOD II $k \times 10^2$ (cm./sec.)
1	a	209.8	3.988	2.525	24.33	0.601	1.261	0.605	1.269
	b	209.2	1.426	0.686	12.10	0.612	1.280	0.613	1.282
2	a	212.4	4.158	3.258	14.97	0.601	1.276	0.603	1.281
	b	208.6	1.690	1.208	7.96	0.606	1.264	0.605	1.269
3	a	210.5	4.739	3.561	19.87	0.593	1.248	0.593	1.248
	b	209.0	2.081	1.447	10.58	0.599	1.252	0.598	1.250
4	—	209.8	6.205	5.090	18.83	0.592	1.242	0.593	1.248
5	a	214.4	3.161	2.170	16.90	0.586	1.256	0.587	1.259
	b	213.6	1.320	0.882	7.34	0.597	1.275	0.597	1.275
						Mean:	1.262		1.265
						Standard Deviation:	0.013		0.014

Figure 5 shows the time-dependence of β_0 and α calculated from the measured values of $x_c\sqrt{c}$ for a number of experimental runs at approximately the same value of $\bar{p}$. Values of k are given in Table II. It is seen that Methods I and II yield virtually the same result and are highly reproducible, the standard deviation being only 1%. As predicted, k is really independent of the bubble size, although air was used as the gas phase.

2. Various Gases through HDTAB Films

Although showing the applicability of the method, the above experiments could not be used to calculate the monolayer permeability from [8] since the film thickness and the solubility and diffusion coefficient of the gas in the liquid phase were not known.

For this reason a 4% solution of hexadecyltrimethylammonium bromide (technical, Eastman Organic Chemicals), which will be referred to as HDTAB, was investigated. The equilibrium film was reached in two clear steps. After the film had drained for some time, a black spot formed at the top and spread over the whole film. Then the film thinned further by the formation of small thicker islands which sank to the bottom after a Brownian-type movement. This thinning in two steps strongly suggested that the final film was a Perrin first-order black film. Since the high transparency of the film also indicated that the film was extremely thin, [10] was assumed to hold. This system had two additional advantages: the film reached the equilibrium thickness within 1 hour after forming the bubble; and the film was highly permeable, so that a complete run never took more than a few hours.

The film permeability was determined for air and seven pure gases: N_2, O_2, H_2, A, Ne, He, and CO_2. Measurements with air, N_2, and O_2 were in triplicate; the values for the other gases are from single experiments. With CO_2 the shrinkage was so rapid that the bubble almost disappeared before the film reached the equilibrium thickness; by tripling the initial bubble volume to 1 ml. it became possible to obtain an acceptable run.

The time dependence of β_0 for some of the gases is shown in Fig. 6. Analysis of the results by Method II revealed that k was initially constant. However, after $x_c\sqrt{c}$ had dropped below approximately 1.6, k apparently decreased in most cases until at the end of the run it was about 10% smaller than the initial value. In all runs with N_2 the drop in k was less pronounced.

A completely satisfactory explanation for this phenomenon has not been found. It may be caused by a small deviation of the bubble shape from the model on which Table I is based, and which assumes that the tension of the film is twice the surface tension of the bulk liquid (11). This assumption may not be exact when the film is extremely thin. We have recalculated the bubble shape for a film tension smaller than twice the surface tension

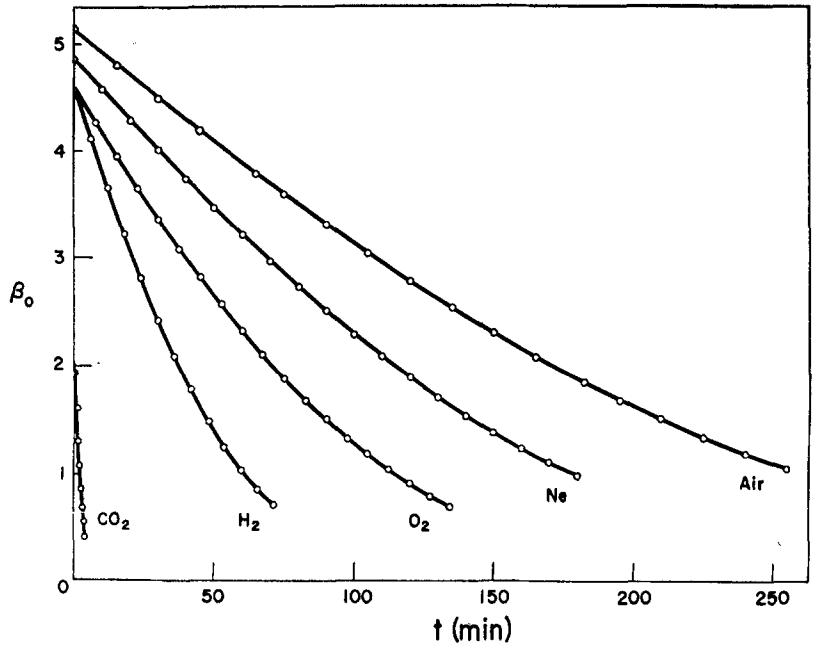

FIG. 6. Time dependence of β_0 for air and some pure gases in the case of a bubble at the surface of a 4% solution of hexadecyltrimethylammonium bromide in water. In the curve for H_2 only half the experimental points are shown.

(12); it is found that when Table I, which would now be inexact, is used an apparent decrease in k occurs as the bubble shrinks. For a reduction in the film tension of 1%, one would find an apparent drop in k of about 10%. This explanation is improbable, however, since the model for a bubble with reduced film tension requires a discontinuity in the slope of the interfaces meeting at the circle of contact (12). But such a discontinuity was never observed. A more likely explanation is the simultaneous presence of a second-order equilibrium film (12); sometimes a vague horizontal boundary was visible between films of different thickness.

The numerical results, which have been collected in Table III, are based on the initial constant value of k; k_{ML} for each gas was calculated from [10] using the H for pure bulk water, although the system is not pure water and H for a very thin liquid film may differ from the value for the bulk liquid. The values of H have been obtained from a variety of sources (16–21); the variation of H with temperature and with the addition of inorganic salts is also assumed to be independent of the presence of the surfactant.

It appears that k_{ML} varies inversely with the collision diameter σ of the gas molecules, especially if one compares similar molecules.

TABLE III

Permeability of Equilibrium Films to Various Gases

Liquid phase: 0.04 g.ml.$^{-1}$ aqueous hexadecyltrimethylammonium bromide

$T = 21.0 \pm 0.05$°C.; $\sqrt{c} = 5.43$ cm.$^{-1}$; $d = 0.999$ g./cm.^{3};

$p_L = 2.5 \times 10^4$ dynes/cm.^{2}

Gas	k (cm./sec.)	$H \times 10^2$	$D \times 10^5$ (cm.^{2}/sec.)	k_{ML} (cm./sec.)	σ (A.)	h^* (A.)
He	0.372	0.94	5.8	79.1	2.16	75
Ne	0.203	1.12	2.8	36.3	2.58	75
A	0.312	3.58	2.0	17.4	3.62	115
H_2	0.576	1.94	5.0	59.3	2.71	85
	0.318					
O_2	0.302	0.308	3.28	2.1	18.8	3.58	110
	0.304					
	0.123					
N_2	0.123	0.123	1.65	2.0	14.9	3.72	135
	0.123					
CO_2	7.55	91.9	1.8	16.4	4.54	110
	0.143					
Air	0.147	0.144				
	0.143					

The collision diameters σ were calculated from gas viscosity data (22, 23).

In its simplest form the energy-barrier theory of monolayer permeation (24, 25) leads to the following equation:

$$k_{ML} = F \exp(-\pi_s a_0/\mathbf{k}T), \qquad [44]$$

where F is a constant, π_s the surface pressure ($= \gamma_{H_2O} - \gamma$), $\mathbf{k}$ the Boltzmann's constant, and a_0 the cross-sectional area of a gas molecule. Since a_0 will be proportional to σ^2, one would expect $\log k_{ML}$ to vary linearly with σ^2 according to:

$$\log_e k_{ML} = \log_e F - \frac{\pi_s a_0}{\mathbf{k}T} = \log_e F - \frac{f\pi_s \sigma^2}{\mathbf{k}T}, \qquad [45]$$

where f is a dimensionless constant.

Figure 7 shows that this relation holds reasonably well for the monatomic and diatomic gases. Since $\pi_s = 39.0$ dynes/cm., F and f in [45] have the approximate values of 180 cm./sec. and 1.90, respectively. CO_2 does not fit into this picture at all; initially it was thought that this resulted from its chemical reaction with water. Subsequent experiments, however, discussed below, revealed that N_2O behaves similarly.

The value of h^* was calculated for those gases which have known diffu-

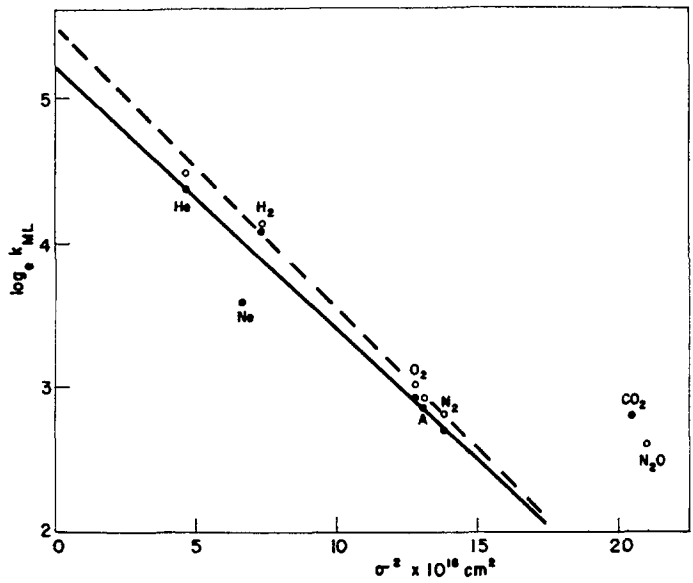

FIG. 7. Relation between the monolayer permeability and the size of the permeating gas molecule, at 21.0°C. for 4% HDTAB (*solid circles*) and 4% HDTAB + 1% NaBr (*open circles*).

sion constants (26, 27), and in all cases was found to be of the order of 100 A. If the monolayer thickness is assumed to be 30 A. (the approximate length of the surfactant molecule), this means that the monolayer is about one-third as permeable as a water film of the same thickness. Actually, the individual values of h^* may be much closer, since the diffusion coefficients D are not very accurately known.

Finally, the results also permit a test of [40]. Since k for argon and oxygen are almost the same, we include argon in the mole fraction of oxygen. With the mole fractions $\bar{x}_{O_2} = 0.220$ and $\bar{x}_{N_2} = 0.780$, [40] predicts

$$k_{air} = \frac{1}{0.220/0.308 + 0.780/0.123} = 0.142 \text{ cm./sec.},$$

which is in good agreement with the experimental value (Table III).

3. *Effect of Electrolytes*

Similar experiments were carried out with H_2, O_2, N_2, He, A, and N_2O in the system 4% HDTAB + 1% NaBr. In contrast to the system without salt k appeared to increase slightly during the first part of a run and then became constant. The initial increase is probably due to continuing drainage after the black film had covered the cap and when the experiment was started. The results are summarized in Table IV, and the dependence of

TABLE IV

Permeability of Equilibrium Films to Various Gases with Added Salt

Liquid Phase: 0.04 g.ml.$^{-1}$ HDTAB + 0.01 g.ml.$^{-1}$ NaBr.

T = 21.0 ± 0.05°C; $\sqrt{c}$ = 5.55 cm.$^{-1}$; d = 1.007 g./cm.^{3}

Gas	k (*cm./sec.*)	$H \times 10^2$ (*est.*)	k_{ML} (*cm./sec.*)	σ (*A.*)
He	0.398	0.90	88.5	2.16
A	0.322	3.43	18.8	3.62
H_2	0.577	1.86	62.0	2.71
O_2	0.321	3.14	20.5	3.58
N_2	0.131[5]	1.58	16.6	3.72
N_2O	4.31	63.5	13.6	4.59

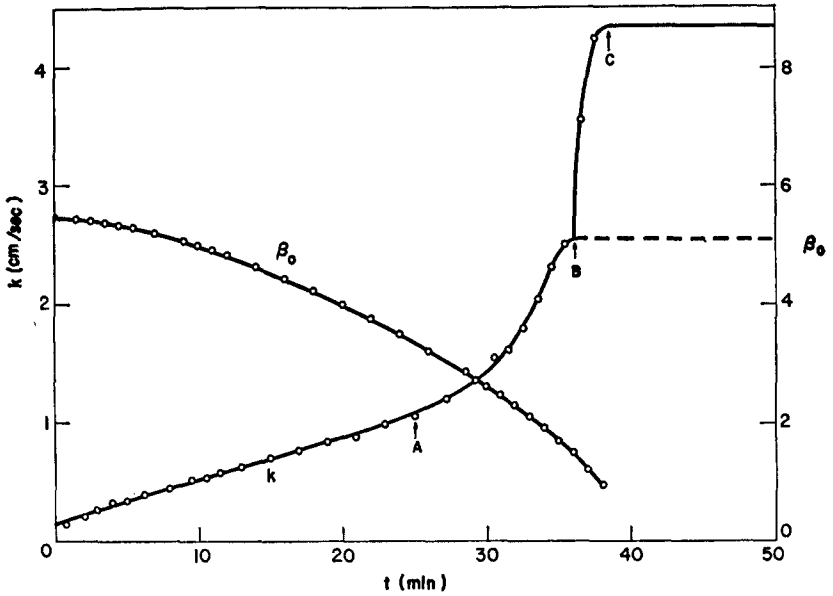

FIG. 8. Time dependence of β_0 and k for N_2O through a draining film in 4% HDTAB + 1% NaBr at 21.0°C.

log k_{ML} on σ^2 is shown in Fig. 7. For the monatomic and diatomic gases slightly higher permeabilities were found than in the system without salt. N_2O was selected as a representative of the triatomic gases because unlike CO_2 it does not react with water; however, it shows the same deviation from the line in Fig. 7.

The high k of N_2O made it possible to study draining films; the time dependence of β_0 and k are shown in Fig. 8. Soon after formation of the bubble, the film was uniform in thickness as indicated by the interference

colors. Initially k increased almost linearly with time until the formation of a black spot at the top of the film (A). At B the black film had covered the whole cap. This film, probably a second-order "equilibrium" film, existed for less than a minute. Then a sudden and extremely rapid thinning of the film took place, accompanied by a fast increase in k toward the equilibrium value at C where $k = 4.31$ cm./sec. and, from [10], $k_{ML} = 13.6$ cm./sec. We estimate that for the second-order film $k = 2.55$ cm./sec. With $D = 1.8 \times 10^{-5}$ cm.^{2}/sec. and $H = 0.635$, Eq. [8] indicates that in this film $h = 190$ A., which seems large at this electrolyte concentration (7).

The film thickness could be estimated from the interference colors during the first 5 minutes only. After 4 minutes the film was approximately 2600 A. thick with a permeability of about 0.30 cm./sec. With the above values of h, D, H, and k_{ML}, Eq. [8] yields $k = 0.40$ cm./sec. This difference seems too large to be accounted for by experimental errors in h or k. A more likely source of errors lies in the estimated values of D and H. Combining Eqs. [8] and [10] leads to

$$k = \frac{DH}{h + DH/k_1}, \qquad [46]$$

where k_1 is the permeability of the Perrin film ($= 4.31$ cm./sec.). With $h = 2.6 \times 10^{-5}$ cm. and $k = 0.30$ cm./sec., Eq. [46] yields $DH = 0.84 \times 10^{-5}$ cm.^{2}/sec., instead of $0.635 \times 1.8 \times 10^{-5}$ which equals 1.14×10^{-5} cm.^{2}/sec. With this value of DH, Eq. [46] leads to $h = 135$ A for the second order film, which seems more reasonable, although still rather high.

This experiment suggests that also in this system the final equilibrium film is a Perrin first-order black film. However, when the NaBr concentration was increased to 10%, the equilibrium film seemed to be slightly more transparent; this may indicate a further thinning.

Table V shows that k is not very sensitive to the addition of salt. If one takes into account the effect of the salt on the gas solubility, k_{ML} appears to increase appreciably.

4. Temperature and Surfactant Concentration

The effect of temperature was studied in the system 4% HDTAB + 1% NaBr. Although the temperature range was small, a considerable increase of k and k_{ML} with temperature was found (Table VI). The effect on k_{ML} is larger than one would expect from [45], even if one takes into account the decrease in σ with temperature.

Varying the concentration of HDTAB in the absence of salt has a small effect on k as long as the concentration is above 0.25%. However, at 0.1% the permeability was very much lower (Table VII); here the film was rigid and slow draining (28) possibly from formation of a monolayer complex between the HDTAB and some impurity in the technical product. The

TABLE V

Effect of Electrolyte on Permeability

O_2 at 21.0°C. through 0.04 g.ml.$^{-1}$ HDTAB

NaBr (g.ml.$^{-1}$)	$\sqrt{c}$ (cm.$^{-1}$)	d (g./cm.^{3})	k (cm./sec.)	$H \times 10^2$ (est.)	k_{ML} (cm./sec.)
0	5.43	0.999	0.308	3.28	18.8
0.01	5.55	1.007	0.321	3.14	20.5
0.10	5.80	1.075	0.315	2.13	29.6

TABLE VI

Effect of Temperature on Permeability

O_2 through 0.04 g.ml.$^{-1}$ HDTAB + 0.01 g.ml.$^{-1}$ NaBr

$\sqrt{c}$ = 5.55 cm.$^{-1}$

T (°C.)	k (cm./sec.)	$H \times 10^2$ (est.)	k_{ML} (cm./sec.)
16.0	0.298	3.45	17.3
21.0	0.321	3.14	20.5
26.0	0.398	2.87	27.8

TABLE VII

Effect of Surfactant Concentration on Permeability

O_2 at 21.0°C.

HDTAB (g. ml.$^{-1}$)	$\sqrt{c}$ (cm.$^{-1}$)	k (cm./sec.)
0.04	5.43	0.308
0.01	5.39	0.295
0.0025	5.40	0.276
0.0010	5.95	0.010

presence of impurities is also indicated by the low value of γ, or high value $\sqrt{c}$, at this concentration. The system behaved similarly to a solution of sodiumdodecylsulfate which contains laurylalcohol as an impurity (28, 29). At higher concentrations the film is mobile or fast draining, although at 0.25 % we sometimes obtained rigid films of low k.

The low value of k in 0.1 % HDTAB may be partly explained by an increase in h, but the main cause is undoubtedly a very low value of k_{ML} due to the formation of the rigid monolayer.

The values in Table VII are not as accurate as those obtained in the previous experiments. In 1 % and 0.25 % HDTAB, k was found to decrease continuously during the whole run; the values reported are the initial values. In 0.1 % the final film always contained some thicker spots and k was not very reproducible.

Concluding Remarks

The experiments reported above show that the method allows accurate measurement of k. In calculating k_{ML} from k, [10] was assumed to hold although this may not be completely valid. For this reason the values of k_{ML} in Tables III, IV, V, and VI are somewhat uncertain. The increase of k_{ML} with the electrolyte concentration (Table V) is contrary to expectation but can be explained if there is a central layer the thickness h of which decreases when electrolyte is added. As an example, if it is assumed that the equilibrium film in 4% HDTAB contains a central liquid layer of $h = 50$ A, k_{ML} for O_2 calculated from [8] is 24.2 cm./sec. instead of 18.8 cm./sec. reported in Tables III and V. Similarly, the large effect of temperature on k_{ML} (Table VI) may be partly caused by a decrease in h with temperature. These examples show that the value of the method can be greatly enhanced if direct measurements of the thickness of the equilibrium film can be made simultaneously. The method could then also be used to determine the diffusion coefficients of gases in water via [9] or [8] by measuring the permeability of thick equilibrium films of known thickness.

In this paper we have emphasized the *permeabilities* of the film and of the monolayers, since they appear logically as proportionality constants in the flux equations [2], [5], and [6]. Alternatively, one can use the inverse quantity "*resistance.*" Then Eq. [8] can be written

$$\frac{1}{k} = \frac{h}{DH} + \frac{2}{k_{ML}H},$$

which shows that the total resistance of the film is the sum of a resistance of the central liquid layer and the resistances of the monolayers. Presented this way, it may appear strange that the latter resistance still contains H; this suggests a slightly different definition of monolayer permeability, namely,

$$k'_{ML} = k_{ML}H.$$

For very thin films, Eq. [10] would then become

$$k = k'_{ML}/2.$$

If this equation is applied to calculate k'_{ML} from k in Tables III and IV, it develops that there is no clear relation between k'_{ML} and the size of the permeating gas molecule.

List of Symbols

a_0 = cross-sectional area of a gas molecule.
A = film area.
b = radius of curvature in the lowest point of the bubble.
c = dg/γ.
C_1, C_2 = gas concentrations outside the film (moles/cm.^{3}).

C_1', C_2' = gas concentrations in the central liquid layer of the film adjacent to the monolayers (moles/cm.^{3}).
$\bar{C}_1$, $\bar{C}_2$ = gas concentrations in the liquid in equilibrium with C_1, C_2 (moles/cm.^{3}).
d = density of the liquid.
D = diffusion coefficient of a gas in the liquid.
f = a_0/σ^2.
F = a constant.
g = acceleration due to gravity.
h = thickness of central liquid layer.
h^* = thickness of a film of bulk liquid with the same permeability as a monolayer.
h_{cap} = height of spherical film.
H = Ostwald coefficient of gas solubility.
k = film permeability.
$\mathbf{k}$ = Boltzmann's constant.
k_{ML} = monolayer permeability.
K = parameter containing k.
N = number of moles of gas.
p, $\bar{p}$ = pressure inside and outside the bubble, respectively.
p_A, $\bar{p}_A$ = partial pressure of component A inside and outside the bubble, respectively.
p_L = vapor pressure of the liquid.
r = radius of a sphere of the same volume as the bubble.
r_0 = radius of spherical bubble at zero time.
R = radius of spherical film.
$\mathbf{R}$ = gas constant.
t = time.
T = absolute temperature.
V = volume of the bubble.
x_A, $\bar{x}_A$ = mole fraction of component A inside and outside the bubble, respectively.
x_c = radius of circle of contact.
Z = subscript indicating either component A or B.
α = h_{cap}/r.
β = cb^2.
β_0 = cr^2.
γ = surface tension.
δ = thickness of monolayer.
π_s = surface pressure.
σ = diameter of gas molecule as calculated from gas viscosity data.

References

1. La Mer, V. K., ed., "Retardation of Evaporation by Monolayers: Transport Processes." Academic Press, New York, (1962).
2. de Vries, A. J., Rec. Trav. Chim. **77,** 209 (1958).
3. de Vries, A. J., *Rec. Trav. Chim.* **77,** 383 (1958).
4. Brown, A. G., Thuman, W. C., and McBain, J. W., *J. Colloid Sci.* **8,** 508 (1953).
5. Blank, M., *In* V. K. LaMer, ed., "Retardation of Evaporation by Monolayers: Transport Processes," p. 75. Academic Press, New York, 1962.
6. Blank, M., *J. Phys. Chem.* **66,** 1911 (1962).
7. Duyvis, E. M., Thesis, Utrecht, 1962.
8. Sheludko, A., *Koninkl. Ned. Akad. Wetenschap. Proc. Ser. B* **65,** 76 (1962).
9. Van Amerongen, G. J., Thesis, Delft, 1943.
10. Korvezee, A. E., and Mol, E. A. J., *J. Polymer Sci.* **2,** 371 (1947).
11. Princen, H. M., *J. Colloid Sci.* **18,** 178 (1963).
12. Princen, H. M., and Mason, S. G. *J. Colloid Sci.* **20,** 156 (1965).
13. Fordham, S., *Proc. Roy. Soc. (London) Ser A.* **194,** 1 (1948).
14. Princen, H. M., and Mason, S. G., J. Colloid Sci. in press (1965).
15. Kuehner, A. L., *J. Chem. Educ.* **25,** 211 (1948).
16. "Handbook of Chemistry and Physics," 40th ed. Chemical Rubber Publishing Co., Cleveland, 1958.
17. Douglas, E., *J. Phys. Chem.* **68,** 169 (1964).
18. Ben Naim, A., and Baer, S., *Trans. Faraday Soc.* **59,** 2735 (1963).
19. Lannung, A., *J. Am. Chem. Soc.* **52,** 68 (1930).
20. Morrison, T. J., and Johnstone, N. B., *J. Chem. Soc.* **1954,** 3441.
21. "International Critical Tables," Vol. III, 1st ed. McGraw-Hill, New York, 1928.
22. Jeans, Sir James, "An Introduction to the Kinetic Theory of Gases," University Press, Cambridge, 1940.
23. Moelwyn-Hughes, E. A., "Physical Chemistry," 2nd ed., p. 610. Pergamon Press, New York, 1961.
24. Langmuir, I., and Langmuir, D., *J. Phys. Chem.* **31,** 1719 (1927).
25. Langmuir, I., and Schaefer, V. J., *J. Franklin Inst.* **235,** 119 (1943).
26. Arnold, J. H., *J. Am. Chem. Soc.* **52,** 3937 (1930).
27. Himmelblau, D. M., *Chem. Rev.* **64,** 527 (1964).
28. Mysels, K. J., Shinoda K., and Frankel, S., "Soap Films: Studies of their Thinning and a Bibliography." Pergamon Press, New York, (1959).
29. Epstein, M. B., Wilson, A., Jakob, C. W., Conroy, L. E., and Ross, J., *J. Phys. Chem.* **58,** 860 (1954).